






Review

Low-Power Wake-Up Receivers for Resilient Cellular Internet of Things

Siyu Wang^{1,*} , Trevor J. Odelberg² , Peter W. Crary¹ , Mason P. Obery¹  and David D. Wentzloff^{1,*} 

¹ Department of Electrical Engineering, University of Michigan, 500 S. State Street, Ann Arbor, MI 48109, USA; pcrary@umich.edu (P.W.C.); mobery@umich.edu (M.P.O.)

² IEEE USA Congressional Fellow, 2001 L St, NW Suite 700, Washington, DC 20036, USA; odelberg@umich.edu

* Correspondence: wsiyu@umich.edu (S.W.); wentzloff@umich.edu (D.D.W.)

Abstract: Smart Cities leverage large networks of wirelessly connected nodes embedded with sensors and/or actuators. Cellular IoT, such as NB-IoT and 5G RedCap, is often preferred for these applications thanks to its long range, extensive coverage, and good quality of service. In these networks, wireless communication dominates power consumption, motivating research on energy-efficient yet resilient and robust wireless systems. Many IoT use cases require low latency but cannot afford high-power radios continuously operating to accomplish this. In these cases, wake-up receivers (WURs) are a promising solution: while the high-power main radio (MR) is turned off/idle, a lightweight WUR is continuously monitoring the RF channel; when it detects a wake-up sequence, the WUR will turn on the MR for subsequent communications. This article provides an overview of WUR hardware design considerations and challenges for 4G and 5G cellular IoT, summarizes the recent 3GPP activities to standardize NB-IoT and 5G wake-up signals, and presents a state-of-the-art WUR chip.

Keywords: wake-up receiver; low-power receiver; Internet of Things; cellular communication; NB-IoT; 5G; 3GPP; energy efficiency



Academic Editors: Maria Luisa Villani and Antonio De Nicola

Received: 9 December 2024

Revised: 1 January 2025

Accepted: 7 January 2025

Published: 13 January 2025

Citation: Wang, S.; Odelberg, T.J.; Crary, P.W.; Obery, M.P.; Wentzloff, D.D. Low-Power Wake-Up Receivers for Resilient Cellular Internet of Things. *Information* **2025**, *16*, 43. <https://doi.org/10.3390/info16010043>

Copyright: © 2025 by the authors. Licensee MDPI, Basel, Switzerland. This article is an open access article distributed under the terms and conditions of the Creative Commons Attribution (CC BY) license (<https://creativecommons.org/licenses/by/4.0/>).

1. Introduction

The Internet of Things enables novel applications such as Smart Cities, industrial automation, smart infrastructure, and environmental monitoring [1–3]. These connected nodes use various wireless standards to communicate with each other, such as ZigBee, Bluetooth, NB-IoT, and LoRa. For Smart City applications, cellular IoT such as LTE-M and NB-IoT is preferred because it leverages existing network infrastructure and is capable of providing reliable, scalable, and secure connectivity. In general, IoT devices deployed for monitoring, measuring, etc., are expected to have a battery life of at least a few years [4]. However, current 5G user equipment (UE) is extremely power hungry: according to a recent 3GPP report [5], 5G devices consume tens of milliwatts in the idle/inactive state and hundreds of milliwatts in the active state. As a result, the battery must be recharged or replaced weekly or daily, which is high-cost and not scalable for energy-constrained IoT nodes. Among device operations, wireless communication dominates system power consumption, far exceeding that of sensing, processing, and actuation in most cases [1]. An energy-efficient wireless system design is needed to prolong battery life, improve user experience, and enable mass deployment.

Figure 1 shows the evolution of power-saving mechanisms of cellular devices [6]. Traditionally, power saving can be achieved via Medium Access Control (MAC) duty-cycling protocols. The device is periodically put to sleep and woken up only to transmit

or receive, for example, through extended discontinuous reception (eDRX) and paging protocols in 4G [7,8] and 5G [9] UEs. During the DRX mode, the UE turns off most of its circuitry to save power and pauses monitoring of the physical downlink control channel (PDCCH), as shown in Figure 2a. To meet the battery life requirements, long eDRX cycles must be used: the eDRX sleep time can be as long as 43 min for devices using LTE-M networks, and three hours for devices using NB-IoT or 5G networks in an idle mode [10]. However, this results in high latency in device response time which is unacceptable in many use cases. For example, in the fire detection and extinguishment use case, fire shutters shall be closed and fire sprinklers shall be turned on by the actuators within 1 to 2 s from the time the fire is detected by sensors [11]. In addition, many cellular radios are complex systems that require ~second(s) to boot up from sleep [5]. The ramp-up/-down time and energy from the duty-cycling operation are therefore nontrivial and will be wasted if the device wakes up and receives no actual data packets.

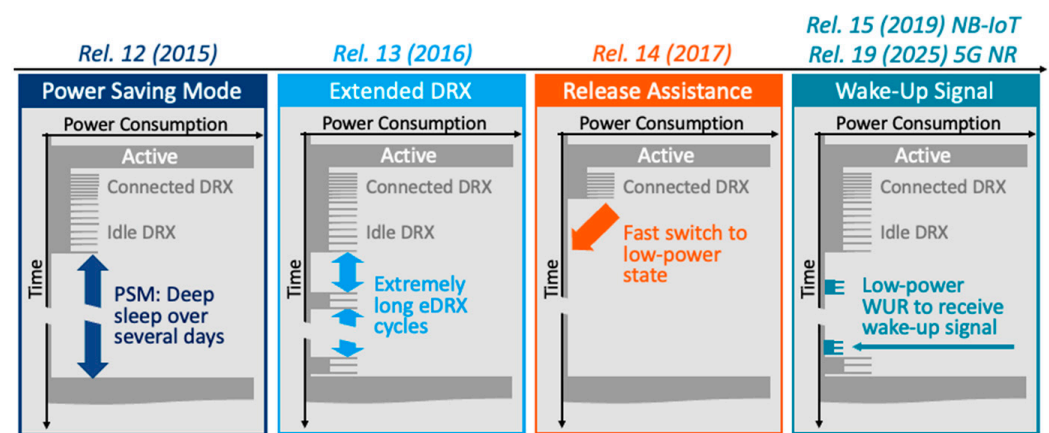


Figure 1. Evolution of cellular device power-saving mechanisms (adapted from [6]).

Alternatively, wake-up radios have recently gained attention as a novel hardware solution to significantly reduce the power and bandwidth while maintaining a low latency. While the high-power main radio (MR) is in sleep mode, a separate lightweight wake-up receiver (WUR) is monitoring the RF spectrum for a wake-up signal (WUS). Upon receiving the WUS from the base station (eNB for NB-IoT and gNB for 5G), the WUR wakes up the MR for subsequent operation including network synchronization and packet transmission. Figure 2b shows a generic architecture of a cellular IoT node with an MR and a WUR, and the corresponding power model assuming a duty-cycled WUR with negligible OFF power consumption. In general, the WUR may reuse some of the MR's hardware components such as the RF matching network, RF front-end filter, and real-time clock (RTC). The WUR can either be always ON or duty-cycled to further save power. In either case, the WUR is expected to periodically synchronize with the base station via synchronization signals (SSs), as shown in Figure 2b. Simulations show that WUR can achieve significant power-saving gain and paging latency reduction compared to the DRX baseline [5]. The power-saving gain can be greater than 90% and 70% for a UE paging probability of 0.1% and 1%, respectively [12].

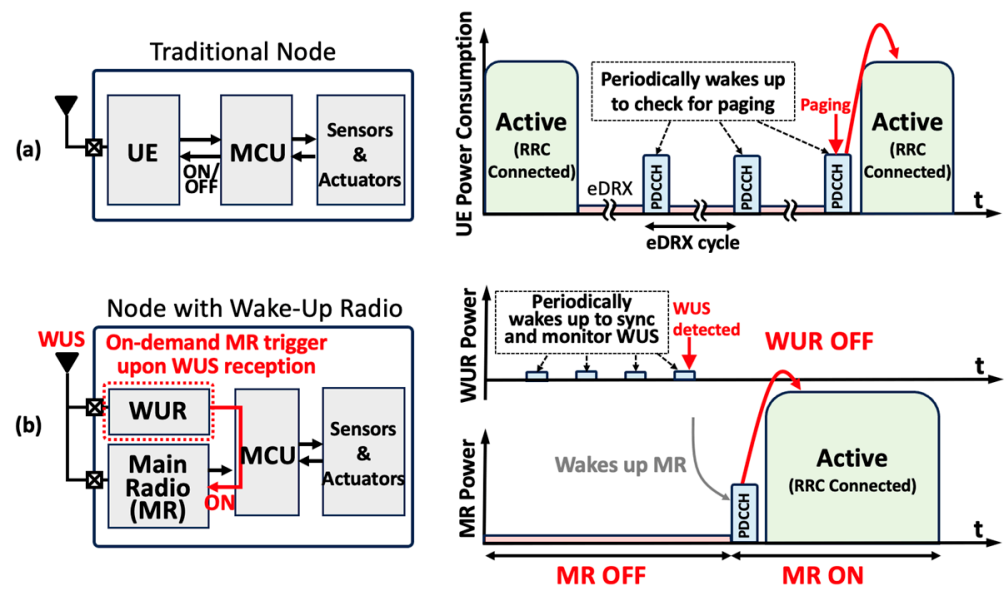


Figure 2. Side-by-side comparison of a traditional eDRX node vs. a node with a WUR. (a) Traditional IoT node structure and power consumption model in eDRX mode. (b) IoT node equipped with WUR and its power consumption model (assuming a duty-cycled WUR).

With the growing popularity of a wake-up signal/wake-up radio for IoT applications, the main purposes of this paper are (1) to fast-track and summarize the recent 3GPP activities on the NB-IoT WUS and the draft 5G LP-WUS/LP-SS (to be included in the 5G standard in 2025), which might be of interest to the cellular IoT community and (2) to discuss the considerations and challenges of cellular WUR design based on recent top IC publications. The remainder of this paper is organized as follows: Section 2 discusses the motivation to standardize WURs for cellular IoT and possible use cases. Section 3 provides an overview of WUR design metrics and requirements. Section 4 summarizes the recent 3GPP activities on standardizing WUR, including the NB-IoT WUR standard introduced in Rel. 15 [13] and the ongoing 5G NR WUR work item for Rel. 19 [11]. Section 5 discusses common receiver architectures suitable for WUR. Section 6 presents the state-of-the-art NB-IoT WUR chips. Section 7 concludes the article.

2. Motivation and Scope of Cellular WURs

Over the past several 3GPP releases, there has been a trend towards reducing device complexity to enable cost-effective deployment of IoT devices, as well as allowing for feature removal when the use case will not benefit. RedCap (reduced capability) devices were introduced in Rel-17, with a 50% to 65% reduction in complexity at a lower data rate still suitable for the most demanding broadband IoT use cases [14]. The introduction of NB-IoT served a similar purpose. Implementing these types of modifications that address a wide range of device capabilities leads to a single standard-based ecosystem and eliminates the choice of radio access technology when planning new IoT deployments or consolidating existing applications to a single technology. Figure 3 provides an illustration of device types for 4G and 5G, with lower data rates corresponding to a distinct reduction in complexity. In each case, a simplified WUR enables a decrease in idle power.

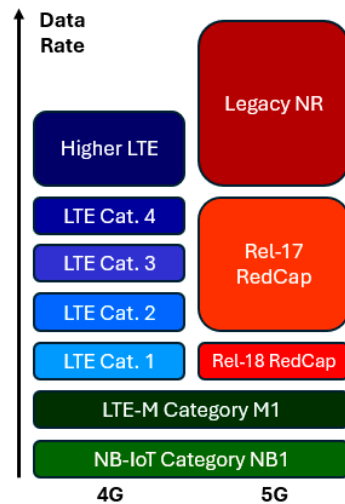


Figure 3. Illustration of 4G and 5G device types (adapted from [14]).

The 3GPP RAN1 group has identified target use cases of WUR under the following three categories: IoT, wearables, and eMBB (enhanced mobile broadband) [5].

The forecasted IoT use cases are notable because they serve functions that should be nearly invisible to the user in the context of Smart Cities. Industrial wireless sensors, controllers, and actuators are all latency-critical. Typically, form factors and power sensitivity will be a function of desired mobility. For example, a static device may be located near existing power infrastructures, excluding the need for energy efficiency. On the other hand, highly mobile cases face power, size, and weight constraints.

Wearable devices including smart watches, rings, and medical monitoring devices benefit from the same overall weight and power reduction, with a somewhat higher target throughput. A similar category, eMBB, is assumed to have a relatively relaxed form factor and comprises personal devices such as smartphones and smart glasses.

Mobile devices used for communication between humans need to check frequently for incoming messages, whereas industrial sensors may only initiate communication when abnormal conditions are detected, such as fire detectors and extinguishers in a building. For the former case, the period may be configured to optimize the user experience. In the latter case, however, eDRX operation is not a good solution. The infrequency of messages calls for very long duty-cycling periods, but in the rare case that a message is sent, it will be very urgent. Another use case, asset tracking, may have a daily or hourly schedule where it regularly reports its current location and status. However, the user may want to reach the device on an infrequent basis, and therefore, it must always be reachable. By employing a WUS, the device can follow its normal behavior with significantly reduced latency as needed.

In general, the addition of wake-up capability provides a highly adaptable technique to adjust latency and simultaneously reduce power consumption compared to the legacy methods based on straightforward UE duty cycling.

3. WUR Performance Metrics and Requirements

While the use of a WUR has promising benefits of reducing system power consumption with low latency, there are several design challenges and tradeoffs that need to be kept in mind. An online survey [15] provides a database of the performance of ultra-low-power (ULP) radios published in top IEEE integrated circuit (IC) conferences and journals since 2005. The database is helpful in analyzing the trends of ULP WUR designs.

1. **Power Consumption:** While the exact power target depends on the specific scenario (MR power, average paging rate, WUR duty-cycling rate, etc.), 3GPP estimates a WUR active power of around 1 mW to achieve a power-saving gain greater than 90% [5,12,16];
2. **Modulation Scheme and Standard Compatibility:** A relatively stringent power budget limits the receiver design complexity, therefore limiting the choice of modulation schemes. Most ultra-low-power WURs in the existing literature only support simple non-coherent modulations, as seen in Figure 4, such as OOK (on-off keying) [17–26], FSK (frequency shift keying) [27–33], or PSK (phase shift keying) [34–38]. However, these modulations have the drawbacks of low throughput and poor bandwidth efficiency. More importantly, they are not compliant with the existing cellular standards and cannot be adopted for wide use. On the other hand, OFDM QPSK/QAM used by 4G/5G are complex modulation schemes that support high data rates but demand more precise receiver designs, resulting in much higher power consumption. This motivates novel WUS designs like multi-carrier OOK [39,40] that can be received and decoded with low-power receivers while being compatible with the existing base station hardware.

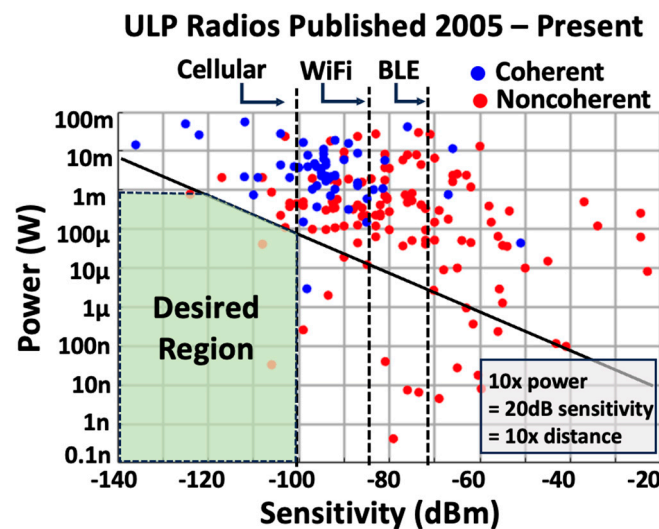


Figure 4. Power vs. sensitivity [15].

3. **Sensitivity and Coverage:** It is desirable to have the WUR achieve the same or better coverage as the MR. Receiver sensitivity, which is the minimum RF signal strength a receiver can reliably detect and decode, is often a direct proxy for communication range. It is expressed as

$$P_{\text{sen}} = -174 \text{ dBm/Hz} + 10\log_{10}(\text{BW}) + \text{NF} + 10\log_{10}(\text{SNR}_{\text{min}}), \quad (1)$$

where BW is the receiver bandwidth, NF is the receiver noise figure (in dB), and SNR_{min} is the minimum signal-to-noise ratio (SNR) required to demodulate the signal with a specified bit error rate (BER). SNR_{min} is determined by the modulation scheme, independent of receiver hardware design. Therefore, a receiver with low NF is required to achieve good sensitivity and wide coverage. However, a fundamental noise–power tradeoff exists, making it very difficult to achieve good NF with low power [15], as seen in Figure 4.

4. **Latency:** In most cases, latency can be defined as the interval between the time of data transmission from the base station and the time that the UE can monitor the paging occasion (PO) [5]. This then includes the WUS on-air time, the delay of the WUR (hardware processing delay and possible delay due to WUR duty cycling and synchronization), and the delay due to MR ramp-up and synchronization.

5. **Interference Resiliency:** Cellular WURs would likely operate alongside congested wireless traffic, where wireless interferers can potentially cause undesirable false wake-ups of WUR nodes. The signal-to-interference ratio (SIR) is a performance metric for a receiver's interference resiliency (a more negative SIR is better). As shown in Figure 5, however, high interference rejection is a challenge for ULP receiver design [15].
6. **Data Rate:** For a given amount of data, a larger data rate means less on-air time, which translates to lower delays and less energy consumption. On the other hand, some applications may require exchanges of large payloads, while others may not. In the former case, it is especially crucial to support a relatively high data rate.
7. **System Impact:** Cellular IoT uses licensed spectra that are costly for service providers. The introduction of WURs should co-exist with legacy signals and cause minimum system overhead to the base stations: this includes time and frequency resource elements (REs) allocated for the WUS, and the impact of WUS on system capacity and base station energy consumption.

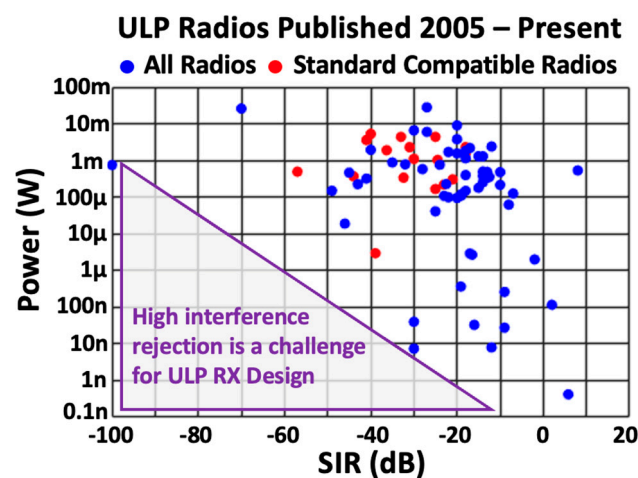


Figure 5. Power vs. SIR (only 79 out of 228 ULP RXs reported SIR) [15].

4. WUR in Cellular Standards

Existing cellular signals employ complex modulation techniques that enable high data throughput but require high-performance and high-power receivers. For example, legacy NB-IoT DL uses OFDM with QPSK, and legacy 5G NR uses OFDM with 64-QAM. Designing a WUS with a simpler modulation scheme can help reduce WUR overhead, but might sacrifice, for example, throughput (data rate) and bandwidth efficiency.

4.1. NB-IoT Wake-Up Signal

Introduced in 3GPP Rel. 15, NB-IoT paging events during extended discontinuous reception (eDRX) operation are prepended by the Narrowband Wake-Up Signal (NWUS) [13]. The NWUS is a short correlation-based sequence that is unique to a certain device or subset of devices. This allows the device to only need to monitor for NWUSs instead of full paging messages while in the idle state. Once the correct NWUS message is received, the device can wake up its main radio to demodulate the following paging message.

Figure 6 shows the frequency–time resource grid and frame structure of LTE/NB-IoT. In the time domain, each 0.5 ms slot contains seven OFDM symbols. In the frequency domain, each resource block (RB) contains 12 consecutive subcarriers. The NWUS is a

132-length complex Zadoff–Chu sequence and is sent in a single 1 ms subframe. The simplified 132-length sequence expression is

$$z_u(n) = e^{\frac{jN_{ID}\pi n(n+1)}{131}} \tag{2}$$

where N_{ID} indicates the group NWUS resource to which the UE is associated. The Zadoff–Chu sequence is encoded into the frequency domain and transmitted via 11 OFDM symbols, each with 12 subcarriers and 15 kHz spacing. The total bandwidth of the NWUS is 180 kHz. As a standard NB-IoT subframe is 14 OFDM symbols, the first 3 symbols of the NWUS are reserved (Figure 7). The NWUS contains a single bit of information, to wake up or not, determined by whether it meets the correlation threshold of the assigned NWUS on the device.

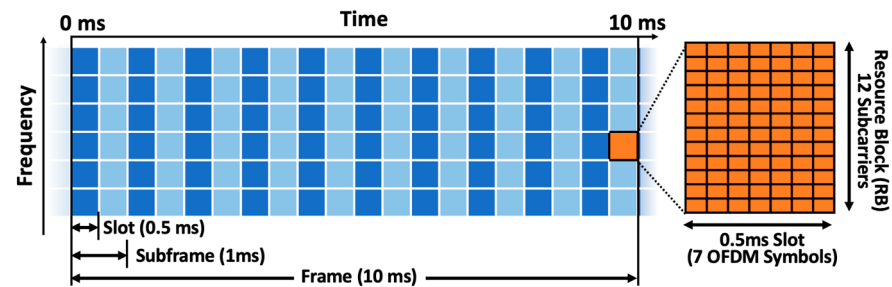


Figure 6. LTE/NB-IoT resource grid, frame structure, and resource block.

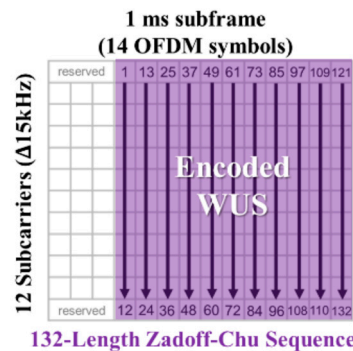


Figure 7. NWUS physical structure.

The use of OFDM requires an FFT for demodulation. As a result, the power of digital baseband processing is often equal to or greater than the power of the receiver front end, with the majority of the power consumed by the FFT [41]. This high power motivates new hardware techniques to reduce the power of NB-IoT radios. In Section 6, we present a state-of-the-art NB-IoT WUR with an integrated digital baseband FFT optimized for NWUS detection.

4.2. Fifth-Generation NR LP-WUS and LP-SS

The 3GPP RAN1 group is currently drafting a 5G wake-up signal standard in a Rel. 19 work item, which consists of the design of two signals: a low-power wake-up signal (LP-WUS) and a low-power synchronization signal (LP-SS) for 5G NR.

4.2.1. LP-WUS

While the technical specifications have not been finalized yet, 3GPP RAN1 has already established several working agreements and assumptions. In addition, 5G also utilizes OFDM and shares a similar resource grid structure as LTE (Figure 6). Urban scenarios are prioritized, with a 30 kHz subcarrier spacing in 4 GHz and 2.6 GHz carrier frequency

bands. The LP-WUS transmission is assumed to occupy 12 RBs, equivalent to a 4.32 MHz bandwidth, in a 20 MHz channel (Figure 8). Additional guard bands can be placed between the LP-WUS and other NR traffic to relax the hardware filtering requirements and improve interference rejection.

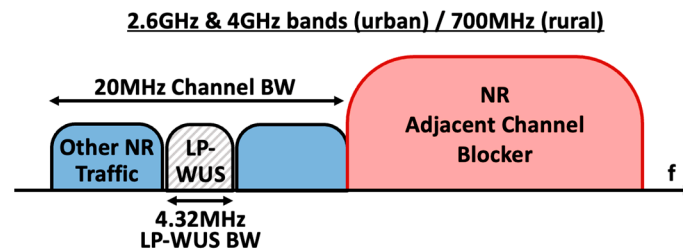


Figure 8. Frequency-domain allocation, assuming a 20 MHz channel BW and a 4.32 MHz LP-WUS BW.

In addition to the wake-up instruction (to wake up the MR or not) and target device ID, the LP-WUS is expected to carry additional information to offload the MR radio resource measurement (RRM) in order to reduce latency. Unlike NWUS, which is a complex Zadoff-Chu sequence and requires a coherent WUR, LP-WUS is designed to emulate on-off keying (OOK) in the time domain to reduce hardware design complexity and relax the power overhead. This is referred to as multi-carrier OOK (MC-OOK) modulation. Figures 9 and 10 illustrate the two proposed mechanisms, namely OOK-1 and OOK-4, used to generate LP-WUS with existing 5G gNB (base station) hardware. Both methods are compatible with existing gNB and would only require a firmware upgrade.

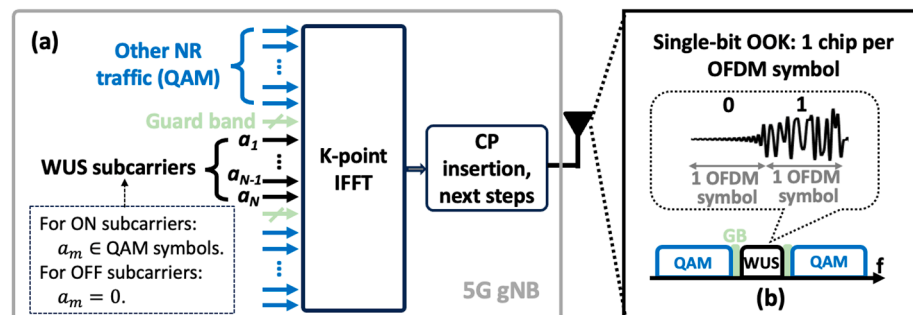


Figure 9. (a) Waveform generation at 5G gNB using the OOK-1 method; (b) the resulting WUS carries 1 information bit (wake up or not) per OFDM symbol.

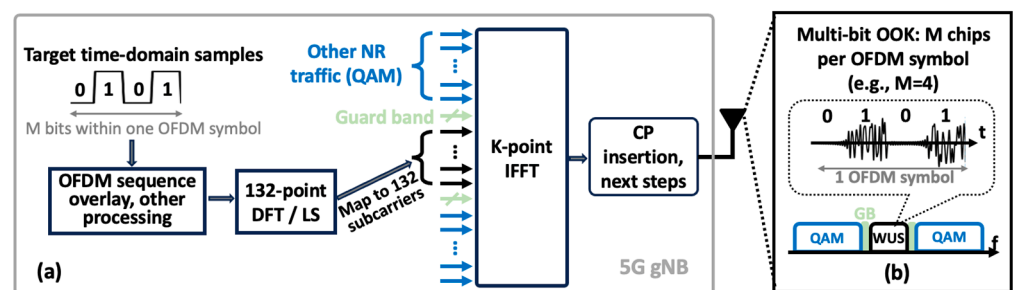


Figure 10. (a) Waveform generation at 5G gNB using the OOK-4 method; (b) the resulting time-domain WUS waveform and channel frequency allocation. With OOK-4, each OFDM symbol contains multiple (M) chips.

OOK-1 is much simpler but only carries one OOK chip per OFDM symbol. On the other hand, OOK-4 poses higher complexity for the gNB but can carry up to four OOK chips within each OFDM symbol, leading to a higher data rate. The 3GPP RAN1 group

is also studying the feasibility of packing more information into the OOK-4 LP-WUS by overlaying each ON chip with an OFDM sequence. The overlaid LP-WUS can be decoded by a high-power OFDM receiver more quickly, potentially saving power through a shorter on-air time.

4.2.2. LP-SS

The LP-SS provides low-power network synchronization required for cellular IoT devices. The signal can be used to correct for frequency drift of the crystal oscillator. Minimizing timing error enables more efficient spectral usage by 5G IoT networks. One of a set of four sequences will be transmitted on the LP-SS with OOK modulation. The four sequences will be used to differentiate neighboring cells.

The WUR turns on for a short period where it will correlate a received OOK signal with a template sequence, which is shorter than one resource block. The four sequences will be selected to maximize synchronization accuracy and will have strong cross-correlation properties in reference to each other. Current candidates for sequences include Gold Codes, m-sequences, and computer-searched sequences [42].

Correlation of the signal can be carried out synchronously or via post-processing, as illustrated in Figure 11. The correlation value during the forecasted frequency error window is used to resynchronize the gNB and the UE. An overlaid OFDM sequence will allow existing MR cellular receivers to use the LP-SS for timing synchronization [43].

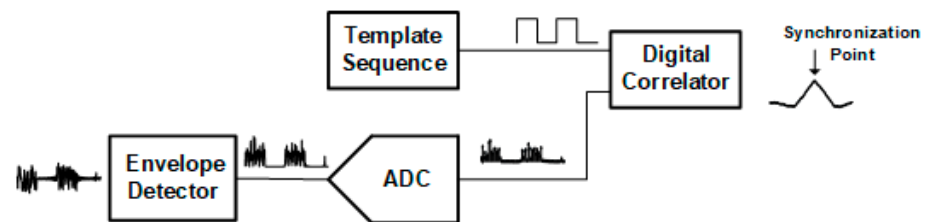


Figure 11. Block diagram for baseband processing of LP-SS signal.

5. Overview of WUR Architectures

Several hardware surveys have discussed low-power receiver design and tradeoffs in extensive detail [1,44,45]. We provide a brief overview of common low-power receiver architectures in this section.

5.1. Conventional Heterodyne OFDM Receiver

Figure 12 shows the architecture of a typical modern heterodyne receiver for cellular communication [46]. Due to the coherent nature of the NB-IoT WUS, it can only be demodulated via a coherent quadrature receiver similar to this. A matching network and a band-select bandpass filter (usually off-chip) provide impedance matching and reject out-of-band blockers.

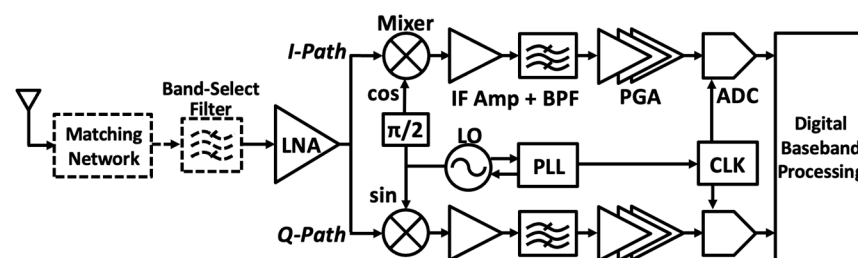


Figure 12. Architecture of a conventional heterodyne receiver.

We identify several power-hungry components as design challenges, which are typically omitted in the ULP receivers in Section 5.2:

1. **Frequency Synthesis:** To demodulate coherent signals such as QAM and QPSK, accurate phase information is needed, necessitating quadrature local oscillator (LO) generation for down conversion and a high-performance phase-locked loop (PLL) to minimize the center frequency offset (CFO) and sampling frequency offset (SFO). These blocks often account for half or more of the total power consumption in many receivers.
2. **Analog-to-Digital Converter (ADC):** Higher-order modulations, such as 64-QAM, require a high-resolution ADC, which is high-power, to digitize the baseband analog signal with sufficient resolution for digital signal processing and demodulation. In addition, according to the Nyquist sampling theorem, a signal with bandwidth B requires a minimum sampling frequency of $2B$. For high-data-rate signals with a large bandwidth, a high clock frequency is required for the ADC, increasing the power overhead. It should be noted that for NWUS, which only occupies a 180 kHz bandwidth, the sampling frequency is significantly relaxed.
3. **Low-Noise Amplifier (LNA):** The LNA is the first stage of the receiver and therefore dominates the noise performance. It must have a good NF to meet stringent sensitivity/coverage requirements. This translates to a high power consumption due to the fundamental power–noise tradeoff. Circuit design techniques can be applied to reduce power consumption, as discussed in Section 5.2.

5.2. ULP OOK WUR

Recent publications have shown several design trends in three popular ULP receiver architectures for OOK-modulated RF signals: (1) passive energy detector (ED) first, (2) passive mixer first, and (3) LNA first. It should be noted that all three architectures are suitable candidates for NR LP-WUR but not for NB-IoT due to NB-IoT WUS complexity.

- **ED first (Figure 13):** ED can be either passive or active. Utilizing an all-passive RF front end, passive ED-first receivers have the lowest power and can achieve nW [47–49]. On the other hand, active EDs [50,51] consume more power and exhibit flicker noise but can achieve higher conversion gain compared to passive EDs. However, since the ED has a wide input bandwidth, these receivers rely on (usually bulky off-chip) filters for selectivity and do not provide multi-band support. The large BW of ED also limits the sensitivity of the architecture to ~ -60 dBm.

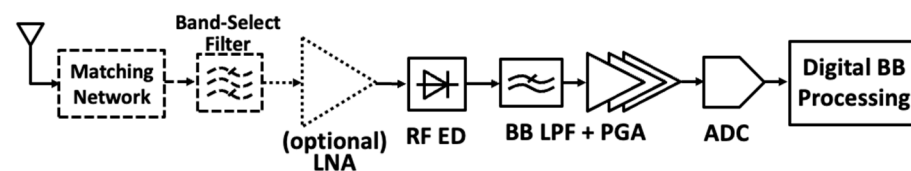


Figure 13. Architecture of an ED-first ULP receiver.

- **Passive mixer first (Figure 14):** Many designs omit the LNA to save power, and instead use a passive mixer, which consumes zero DC power, as the first stage [52,53]. An ED is often placed before the ADC to limit signal bandwidth and thereby relax the sampling requirement. Thanks to their frequency translation property [54,55], passive mixer-first receivers offer good selectivity by simply adjusting the LO frequency. However, due to the lack of RF gain, passive mixer-first receivers have high NF when optimized for low power which degrades the sensitivity performance. The architecture can achieve a decent sensitivity level (~ -80 to -90 dBm) with a sub-mW budget.

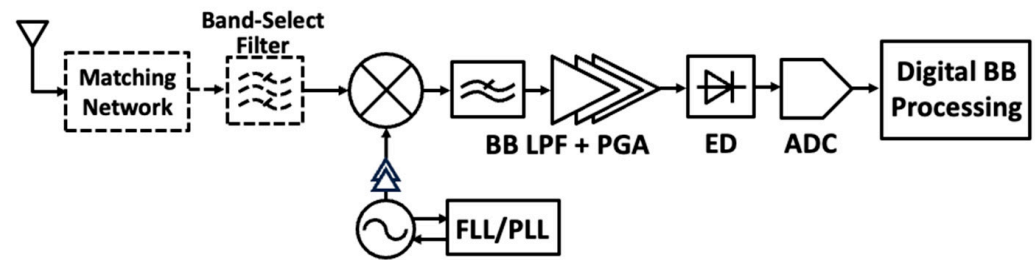


Figure 14. Architecture of a passive mixer-first ULP receiver.

- LNA first (Figure 15): Using an LNA as the first stage significantly improves noise performance and is usually used for good sensitivity performance (< -100 dBm) for long range. However, the LNA can often consume several hundred μ W or more. Several circuit design techniques have been demonstrated to reduce LNA power consumption, including bit-level duty cycling [56], the use of low supply voltages [57], subthreshold operation [58], and current-reuse topology [59].

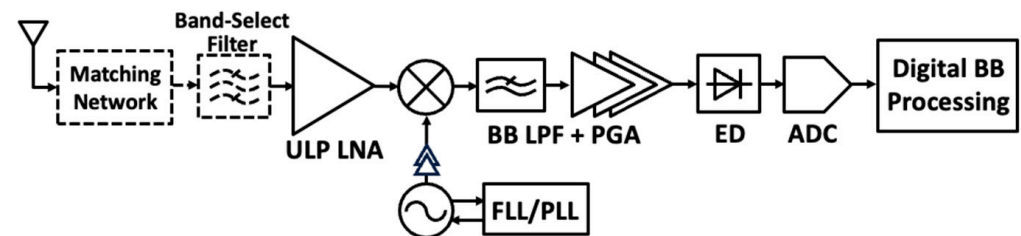


Figure 15. Architecture of an LNA-first ULP receiver.

6. State-of-the-Art NB-IoT WUR

In this section, we present a state-of-the-art standard-compatible NB-IoT WUR with a receiver front end and an integrated digital baseband [60]. The chip was fabricated in 28 nm CMOS, successfully demonstrated on-chip Narrowband Wake-Up Signal (NWUS) demodulation and wake-up detection, and achieved a -107 dBm sensitivity with 2.4 mW power consumption. Overall, the presented chip achieves the highest degree of integration for an NB-IoT WUR and is the first fully standalone solution with on-chip digital processing.

6.1. WUR RF Front End

Figure 16 shows the block diagram of the WUR. The WUR is designed to efficiently receive and process the NWUS as specified in Rel. 15 of the 3GPP standard. The receiver front end utilizes a low-noise transconductance amplifier (LNTA)-first low-IF architecture. A low IF is preferred over direct conversion to reduce the center frequency offset (CFO) effects as well as flicker noise on subcarriers near DC. An oscillator, a fractional-N phase-locked loop (PLL), and a 25% duty-cycle generator are implemented to generate the local oscillator (LO) signal. For each of the I/Q paths, the WUR RF front-end consists of an active mixer, a complex filter, a bandpass filter (BPF), a programmable-gain amplifier (PGA), and a successive-approximation analog-to-digital converter (SAR ADC). The RF front end operates in the RF frequency range of 750–960 MHz and converts the signal to a low IF of 360 kHz.

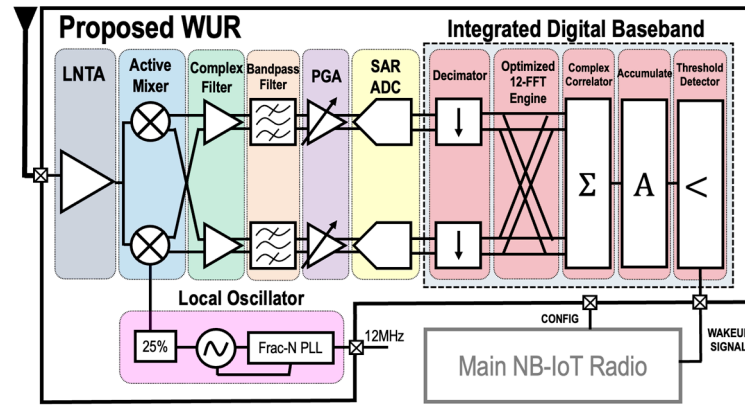


Figure 16. Block diagram of fabricated WUR with integrated digital backend.

An optimized LNTA is followed by active mixers to down-convert and generate quadrature IF signals. Second-order complex poly-phase filters provide bandpass filtering and reject the image frequency. A frequency synthesizer consisting of a fine-step fractional-N PLL and low-power LC-VCO allows for tuning over a wide range of input frequencies. The phase noise of the LC-VCO can be relaxed to save power thanks to the lower SNR requirement of the correlation-based NWUS. The 8-bit SAR ADCs operate at 1.4 MS/s for an oversample rate of $\sim 4\times$. This allows an increase of ~ 6 dB of SNDR (~ 1 ENOB) to the ADC output.

6.2. NWUS Demodulation and Detection

As discussed in Section 4.1, the NB-IoT NWUS is a 132-length Zadoff–Chu correlation sequence encoded into 11 OFDM symbols at a symbol period of 66.7 μs . The NWUS occupies 12 subcarriers with 15 kHz spacing for a total bandwidth of 180 kHz. To decode the NWUS, an FFT is required to convert the Zadoff–Chu sequence to the frequency domain, which is then correlated with a stored NWUS on-chip template. To reduce the high power overhead of the FFT engine seen in other OFDM systems, for this chip, a custom digital baseband utilizing a 12-point FFT is designed and optimized for the NWUS.

Traditionally, data padding is used to convert the FFT into a more traditional Cooley–Tukey radix-2 16-point FFT. However, this work introduces a 12-point FFT (Figure 17) that is more power- and area-efficient for decoding the NWUS.

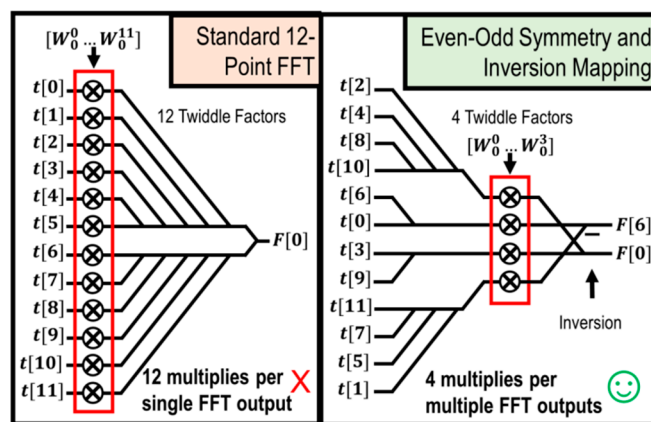


Figure 17. The optimized 12-point FFT. Through exploiting even–odd symmetry and inverting operations, the number of multipliers can be reduced.

Four key design considerations are taken to reduce area and power. First, as a single WUS symbol contains 12 subcarriers, the FFT is chosen to be 12-point which allows for no

data padding, eliminating unnecessary multipliers. Second, the 12-point FFT is performed on a single clock cycle with a fixed-point precision of 16 bits to reduce area overhead from pipeline registers. This is possible given the relatively slow symbol rate of the NWUS, allowing for a slower clock speed. Third, even–odd symmetry mapping is applied to the twiddle factors, reducing the number of multipliers needed per FFT output from 12 to 4. Fourth, inversion mapping is applied to the FFT calculations, which exploits the fact that many calculations differ by only the sign of the operations. This allows for simple data inverters to be used rather than additional multipliers. In total, the total number of complex multipliers needed is 48 per FFT, 25% less than that needed for a 16-point FFT. Table 1 compares the performance of different FFT engine architectures. The optimized 12-point FFT including twiddle factor LUTs occupies only $72 \mu\text{m}^2$ of area and consumes $4 \mu\text{W}$ while clocked at 1.4 MHz.

Table 1. Comparison of different FFT architectures.

	Traditional 12-Point DFT	Pipelined Cooley–Tukey 16-Point FFT	Optimized 12-Point FFT
Number of Complex Multipliers per FFT	144	64	48
Number of Twiddle Factors	144	16	16
Area Estimate	$144 \mu\text{m}^2$	$85 \mu\text{m}^2$	$72 \mu\text{m}^2$
Power Estimate (Normalized)	8.57 pJ/cycle	3.58 pJ/cycle	2.86 pJ/cycle

After the FFT, the data are correlated against an on-chip programmable NWUS template and trigger a wake-up request if a correlation threshold is reached. The correlator has a length of 12 using 16-point precision and accumulates each FFT output over 11 symbols to correlate the entire 132-length Zadoff–Chu NWUS sequence. The accumulation threshold for the NWUS is adjustable given channel conditions to ensure robust tolerance to false detections. The accumulator and threshold detector also support data repetitions to increase processing gain to achieve higher sensitivity as allowed by the NB-IoT standard. However, repetition-less data are reported for this work.

6.3. Experimental Results

The WUR was fabricated in 28 nm CMOS. It occupies an area of 2 mm^2 and consumes 2.4 mW. Figure 18 shows the power breakdown. The digital wake-up processor consumes $27 \mu\text{W}$ and the ADCs consume $30 \mu\text{W}$ each, in total contributing only 4% of the total WUR power.

Measured Power Breakdown

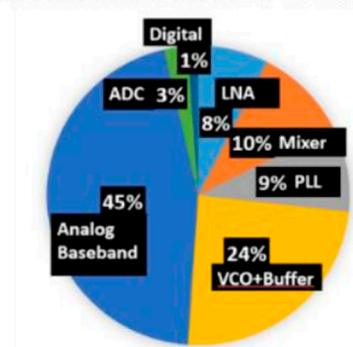


Figure 18. Power breakdown of the NB-IoT WUR.

Figure 19 shows the test setup. An Agilent power supply was used to provide supply voltages to the WUR chip. An Agilent function generator was used to provide a 12 MHz reference clock signal for the on-chip PLL. A Keysight noise source and a Keysight signal analyzer were used for noise figure (NF) measurement. A Tektronix oscilloscope was used to observe the chip output. The RF front-end NF was measured to be 6 dB over the 750–960 MHz RF input. Standard specified NWUS sequences (discussed in Section 4.1) were used to measure the required SNR_{min} of the digital baseband detector. The measured NF and SNR_{min} result in a sensitivity of -107 dBm according to Equation (1).

Figure 19 shows the test setup and the measured WUR output. Two different input signals were tested: the “correct” WUS is a 132-length Zadoff–Chu sequence specified by the 3GPP standard [13], while the “incorrect” WUS is a 132-length random sequence that is not supposed to wake up an NB-IoT WUR. Upon receiving the correct NWUS input, the WUR successfully detected it and sent a wake-up instruction to the main radio (in Figure 19, the orange signal goes high). The incorrect NWUS, on the other hand, did not trigger the WUR wake-up response (Figure 19).

Figure 20 compares the power–sensitivity performance of the presented WUR with other state-of-the-art ULP radios that support coherent modulation schemes. It is one of the lowest-power receivers with a sensitivity greater than -100 dBm. It is also the only integrated NB-IoT WUR with on-chip WUS detection.

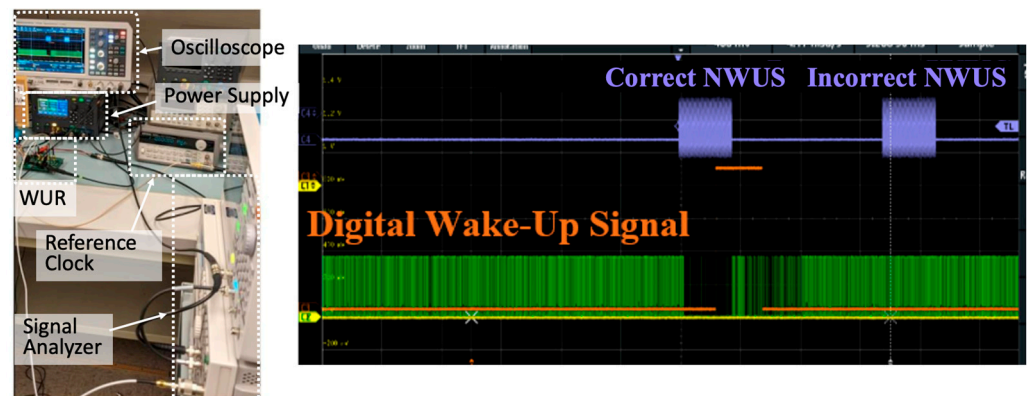


Figure 19. Test setup (left) and measured wake-up event (right).

Coherent ULP Radios Published 2005– Present

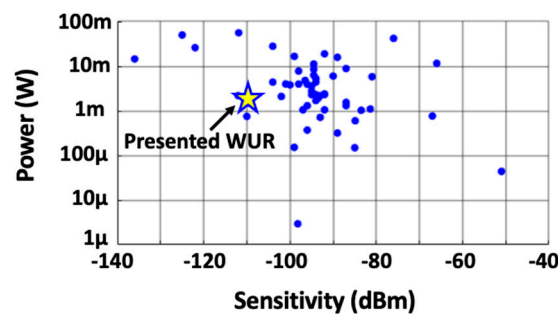


Figure 20. Power vs. sensitivity performance of the presented NB-IoT WUR (starred) compared to other receivers supporting coherent modulation schemes (blue dots).

7. Conclusions

A wake-up radio is a promising solution for energy-efficient cellular IoT applications like Smart Cities. In this paper, an overview of recent 3GPP activities on standardizing NB-IoT and 5G wake-up signals is presented. Wake-up receiver performance tradeoffs and

recent research trends in ultra-low-power receiver designs are discussed. A state-of-the-art fully integrated NB-IoT wake-up receiver is presented. The wake-up receiver achieves a good communication range (-107 dBm sensitivity) with a total power consumption of 2.4 mW.

While there have been significant advancements in ULP radios, the design of high-performance and standard-compliant ULP radios remains a big challenge. Such a challenge must be addressed in order to enable massive deployment and resilient operation of cellular IoT. Future research directions include circuit-level novelties as well as signaling-hardware co-design to alleviate the hardware requirements.

Author Contributions: S.W. was the lead author of the paper and was primarily responsible for drafting the manuscript. S.W., P.W.C., M.P.O. and D.D.W. reviewed, documented, and summarized key documents related to recent 3GPP RAN1 activities on 5G WUS standardization. Similarly, T.J.O. and D.D.W. carried out such activities for NB-IoT. T.J.O. was also the lead designer of the NB-IoT WUR chip presented in this paper. D.D.W. provided project supervision and helped refine the manuscript. All authors have read and agreed to the published version of the manuscript.

Funding: This research received no external funding.

Institutional Review Board Statement: Not applicable.

Informed Consent Statement: Not applicable.

Data Availability Statement: The data presented in this study are available upon request from the corresponding author.

Conflicts of Interest: The authors declare no conflicts of interest.

References

1. Piyare, R.; Murphy, A.L.; Kiraly, C.; Tosato, P.; Brunelli, D. Ultra Low Power Wake-Up Radios: A Hardware and Networking Survey. *IEEE Commun. Surv. Tutor.* **2017**, *19*, 2117–2157. [CrossRef]
2. Rashid, B.; Rehmani, M.H. Applications of wireless sensor networks for urban areas: A survey. *J. Netw. Comput. Appl.* **2016**, *60*, 192–219. [CrossRef]
3. Lea, R.; Blackstock, M. Smart Cities: An IoT-centric Approach. In Proceedings of the 2014 International Workshop on Web Intelligence and Smart Sensing (IWWISS'14), Saint Etienne, France, 1–2 September 2014; Association for Computing Machinery: New York, NY, USA, 2014; pp. 1–2. [CrossRef]
4. Study on Support of Reduced Capability NR Devices, 3GPP Std. TR 38.875. Available online: https://www.3gpp.org/ftp/Specs/archive/38_series/38.875/38875-h00.zip (accessed on 9 December 2024).
5. Study on Low-Power Wake-Up Signal and Receiver for NR, 3GPP Std. TR 38.869. Available online: https://www.3gpp.org/ftp/Specs/archive/38_series/38.869/38869-i00.zip (accessed on 9 December 2024).
6. Rohde & Schwarz. Let's Talk IoT—Low Power Consumption with the Wake-Up Signal (WUS). Available online: https://www.rohde-schwarz.com/se/knowledge-center/videos/let-s-talk-iot-low-power-consumption-with-the-wake-up-signal-wus-video-detailpage_251220-819206.html (accessed on 9 December 2024).
7. LTE Paging in Extended DRX; 3GPP Std. TS36.304, Section 7.3. Available online: https://www.3gpp.org/ftp/Specs/archive/36_series/36.304/36304-i20.zip (accessed on 9 December 2024).
8. LTE Discontinuous Reception (DRX); 3GPP Std. TS 36.321, Section 5.7. Available online: https://www.3gpp.org/ftp/Specs/archive/36_series/36.321/36321-i30.zip (accessed on 9 December 2024).
9. Radio Resource Control (RRC) Protocol Specification, 3GPP Std. TS 38.331. Available online: https://www.3gpp.org/ftp/Specs/archive/38_series/38.331/38331-i30.zip (accessed on 9 December 2024).
10. Liberg, O.; Sundberg, M.; Wang, E.; Bergman, J.; Sachs, J.; Wikström, G. *Cellular Internet of Things: From Massive Deployments to Critical 5G Applications*; Academic Press: Cambridge, MA, USA, 2019.
11. Low-Power Wake-Up Signal and Receiver for NR (LP-WUS/WUR); 3GPP Work Item Description, RP-241824. 2024. Available online: https://www.3gpp.org/ftp/TSG_RAN/TSG_RAN/TSGR_105/Docs/RP-241824.zip (accessed on 9 December 2024).
12. Huang, K.-K.; Luna, R.; Wentzloff, D.D.; Rathonyi, B.; Wang, Y.-P.E.; Chen, J.; Korhonen, J.; Tiri, H.L. NB-IoT Power-Saving Analysis with Wake-Up Signal and Wake-Up Receiver Implementation. In Proceedings of the 2024 IEEE International Conference on Communications Workshops (ICC Workshops), Denver, CO, USA, 9–13 June 2024; pp. 1121–1126. [CrossRef]

13. Narrowband Wake Up Signal Downlink; 3GPP Std. TS 36.211, Section 10.2. Available online: https://www.3gpp.org/ftp/Specs/archive/36_series/36.211/36211-i01.zip (accessed on 9 December 2024).
14. Ericsson. RedCap—Expanding the 5G Device Ecosystem for Consumers and Industries [White Paper]. 2023. Available online: <https://www.ericsson.com/en/reports-and-papers/white-papers/redcap-expanding-the-5g-device-ecosystem-for-consumers-and-industries#:~:text=The%20value%20range%20for%20eDRX,devices%20in%20RRC%20inactive%20mode> (accessed on 9 December 2024).
15. Wentzloff, D.D. Low Power Radio Survey. Available online: www.eecs.umich.edu/wics/low_power_radio_survey.html (accessed on 9 December 2024).
16. Höglund, A.; Mozaffari, M.; Yang, Y.; Moschetti, G.; Kittichokechai, K.; Nory, R. 3GPP Release 18 Wake-Up Receiver: Feature Overview and Evaluations. *IEEE Commun. Stand. Mag.* **2024**, *8*, 10–16. [[CrossRef](#)]
17. Ren, H.; Lyu, L.; Chen, B.; Shi, C.-J.R. A -104dBm-Sensitivity Receiver with Shared Wireless LO and Envelope-Tracking Mixer Achieving -46dB SIR. In Proceedings of the 2024 IEEE Custom Integrated Circuits Conference (CICC), Denver, CO, USA, 21–24 April 2024; pp. 1–2. [[CrossRef](#)]
18. Sun, J.; Yang, C.; Luo, Y.; Dong, S.; Zhao, B. An Interference-Resilient 120-Degree-Apart Pseudo-I/Q BLE-Compliant Wake-Up Receiver Achieving -21dB SIR, -94dBm Sensitivity, and 4-D Wake-Up Signature. In Proceedings of the 2024 IEEE Custom Integrated Circuits Conference (CICC), Denver, CO, USA, 21–24 April 2024; pp. 1–2. [[CrossRef](#)]
19. Lukas, C.J.; Yahya, F.B.; Huang, K.K.; Boley, J.; Truesdell, D.S.; Breiholz, J.; Wokhlu, A.; Craig, K.; Brown, J.K.; Fitting, A.; et al. 15.2 A 2.19 μ W Self-Powered SoC with Integrated Multimodal Energy Harvesting, Dual-Channel up to -92dBm WRX and Energy-Aware Subsystem. In Proceedings of the 2023 IEEE International Solid-State Circuits Conference (ISSCC), San Francisco, CA, USA, 19–23 February 2023; pp. 238–240. [[CrossRef](#)]
20. Huang, K.-K.; Brown, J.K.; Collins, N.; Sawyer, R.K.; Yahya, F.B.; Wang, A.; Roberts, N.E.; Calhoun, B.H.; Wentzloff, D.D. 21.3 A Fully Integrated 2.7 μ W -70.2dBm-Sensitivity Wake-Up Receiver with Charge-Domain Analog Front-End, -16.5dB-SIR, FEC and Cryptographic Checksum. In Proceedings of the 2021 IEEE International Solid-State Circuits Conference (ISSCC), San Francisco, CA, USA, 13–22 February 2021; pp. 306–308. [[CrossRef](#)]
21. Sharemi, H.J.; Bakhtiar, M.S. A 12.2 μ W Interference Robust Wake-Up Receiver. In Proceedings of the 2023 IEEE Custom Integrated Circuits Conference (CICC), San Antonio, TX, USA, 23–26 April 2023; pp. 1–2. [[CrossRef](#)]
22. Bassirian, P.; Duvvuri, D.; Truesdell, D.S.; Liu, N.; Calhoun, B.H.; Bowers, S.M. 30.1 A Temperature-Robust 27.6nW -65dBm Wakeup Receiver at 9.6GHz X-Band. In Proceedings of the 2020 IEEE International Solid-State Circuits Conference—(ISSCC), San Francisco, CA, USA, 16–20 February 2020; pp. 460–462. [[CrossRef](#)]
23. Mangal, V.; Kinget, P.R. 28.1 A 0.42nW 434MHz -79.1dBm Wake-Up Receiver with a Time-Domain Integrator. In Proceedings of the 2019 IEEE International Solid-State Circuits Conference—(ISSCC), San Francisco, CA, USA, 17–21 February 2019; pp. 438–440. [[CrossRef](#)]
24. Mangal, V.; Kinget, P.R. A -80.9dBm 450MHz Wake-Up Receiver with Code-Domain Matched Filtering using a Continuous-Time Analog Correlator. In Proceedings of the 2019 IEEE Radio Frequency Integrated Circuits Symposium (RFIC), Boston, MA, USA, 2–4 June 2019; pp. 259–262. [[CrossRef](#)]
25. Moody, J.; Gong, S.; Calhoun, B.H.; Bowers, S.M.; Dissanayake, A.; Bishop, H.; Lu, R.; Liu, N.; Duvvuri, D.; Gao, A.; et al. A Highly Reconfigurable Bit-Level Duty-Cycled TRF Receiver Achieving -106-dBm Sensitivity and 33-nW Average Power Consumption. *IEEE Solid-State Circuits Lett.* **2019**, *2*, 309–312. [[CrossRef](#)]
26. Rekhi, A.S.; Arbabian, A. A 14.5mm² 8nW -59.7dBm-sensitivity ultrasonic wake-up receiver for power-, area-, and interference-constrained applications. In Proceedings of the 2018 IEEE International Solid-State Circuits Conference—(ISSCC), San Francisco, CA, USA, 11–15 February 2018; pp. 454–456. [[CrossRef](#)]
27. Bishop, H.L.; Dissanayake, A.; Bowers, S.M.; Calhoun, B.H. 21.5 An Integrated 2.4GHz -91.5dBm-Sensitivity Within-Packet Duty-Cycled Wake-Up Receiver Achieving 2 μ W at 100ms Latency. In Proceedings of the 2021 IEEE International Solid-State Circuits Conference (ISSCC), San Francisco, CA, USA, 13–22 February 2021; pp. 310–312. [[CrossRef](#)]
28. Kim, K.-M.; Choi, K.-S.; Jung, H.; Yun, B.; Kim, S.; Oh, W.; Lee, E.-S.; Park, S.; Jeong, E.-R.; Ko, J.; et al. An LPWAN Radio with a Reconfigurable Data/Duty-Cycled-Wake-Up Receiver. In Proceedings of the 2022 IEEE International Solid-State Circuits Conference (ISSCC), San Francisco, CA, USA, 20–26 February 2022; pp. 404–406. [[CrossRef](#)]
29. Thijssen, B.J.; Klumperink, E.A.M.; Quinlan, P.; Nauta, B. 30.4 A 370 μ W 5.5dB-NF BLE/BT5.0/IEEE 802.15.4-Compliant Receiver with >63dB Adjacent Channel Rejection at >2 Channels Offset in 22nm FDSOI. In Proceedings of the 2020 IEEE International Solid-State Circuits Conference—(ISSCC), San Francisco, CA, USA, 16–20 February 2020; pp. 466–468. [[CrossRef](#)]
30. Chang, Z.; Xiao, Q.; Wang, W.; Luo, Y.; Zhao, B. A Passive Bidirectional BLE Tag Demonstrating Battery-Free Communication in Tablet/Smartphone-to-Tag, Tag-to-Tablet/Smartphone, and Tag-to-Tag Modes. In Proceedings of the 2023 IEEE International Solid-State Circuits Conference (ISSCC), San Francisco, CA, USA, 19–23 February 2023; pp. 468–470. [[CrossRef](#)]

31. Wang, P.-H.P.; Mercier, P.P. 28.2 A 220 μ W -85dBm Sensitivity BLE-Compliant Wake-up Receiver Achieving -60dB SIR via Single-Die Multi-Channel FBAR-Based Filtering and a 4-Dimensional Wake-Up Signature. In Proceedings of the 2019 IEEE International Solid-State Circuits Conference—(ISSCC), San Francisco, CA, USA, 17–21 February 2019; pp. 440–442. [[CrossRef](#)]
32. Maksimovic, F.; Wheeler, B.; Burnett, D.C.; Khan, O.; Mesri, S.; Suci, I.; Lee, L.; Moreno, A.; Sundararajan, A.; Zhou, B.; et al. A Crystal-Free Single-Chip Micro Mote with Integrated 802.15.4 Compatible Transceiver, sub-mW BLE Compatible Beacon Transmitter, and Cortex M0. In Proceedings of the 2019 Symposium on VLSI Circuits, Kyoto, Japan, 9–14 June 2019; pp. C88–C89. [[CrossRef](#)]
33. Bae, J.; Yoo, H.-J. A 45 μ W Injection-Locked FSK Wake-Up Receiver With Frequency-to-Envelope Conversion for Crystal-Less Wireless Body Area Network. *IEEE J. Solid-State Circuits* **2015**, *50*, 1351–1360. [[CrossRef](#)]
34. Shen, J.; Zhu, F.; Liu, Y.; Liu, B.; Shi, C.; Huang, L.; Xu, L.; Tian, X.; Zhang, R. 23.1 A 44 μ W IoT Tag Enabling 1 μ s Synchronization Accuracy and OFDMA Concurrent Communication with Software-Defined Modulation. In Proceedings of the 2024 IEEE International Solid-State Circuits Conference (ISSCC), San Francisco, CA, USA, 18–22 February 2024; pp. 400–402. [[CrossRef](#)]
35. Ji, X.; Zhao, J.; Rhee, W.; Wang, Z. A 2.3nJ/b 32-APSK Polar Phase-Tracking Receiver with Two-Point Injection Technique. In Proceedings of the 2024 IEEE Radio Frequency Integrated Circuits Symposium (RFIC), Washington, DC, USA, 16–18 June 2024; pp. 115–118. [[CrossRef](#)]
36. Bialek, H.; Johnston, M.; Natarajan, A. 31.8 A 0.4-to-0.95GHz Distributed N-Path Noise-Cancelling Ultra-Low-Power RX with Integrated Passives Achieving -85dBm/100kb/s Sensitivity, -41dB SIR and 174dB RX FoM in 22nm CMOS. In Proceedings of the 2023 IEEE International Solid-State Circuits Conference (ISSCC), San Francisco, CA, USA, 19–23 February 2023; pp. 474–476. [[CrossRef](#)]
37. Ye, D.; van der Zee, R.; Nauta, B. 26.2 An Ultra-Low-Power receiver using transmitted-reference and shifted limiters for in-band interference resilience. In Proceedings of the 2016 IEEE International Solid-State Circuits Conference (ISSCC), San Francisco, CA, USA, 31 January–4 February 2016; pp. 438–439. [[CrossRef](#)]
38. Vidojkovic, M.; Huang, X.; Wang, X.; Zhou, C.; Ba, A.; Lont, M.; Liu, Y.-H.; Harpe, P.; Ding, M.; Busze, B.; et al. 9.7 A 0.33nJ/b IEEE802.15.6/proprietary-MICS/ISM-band transceiver with scalable data-rate from 11kb/s to 4.5Mb/s for medical applications. In Proceedings of the 2014 IEEE International Solid-State Circuits Conference Digest of Technical Papers (ISSCC), San Francisco, CA, USA, 9–13 February 2014; pp. 170–171. [[CrossRef](#)]
39. *IEEE Std 802.11ba-2021 (Amendment to IEEE Std 802.11-2020 as amendment by IEEE Std 802.11ax-2021, and IEEE Std 802.11ay-2021); IEEE Standard for Information Technology—Telecommunications and Information Exchange between Systems—Local and Metropolitan Area Networks-Specific Requirements—Part 11: Wireless LAN Medium Access Control (MAC) and Physical Layer (PHY) Specifications—Amendment 3: Wake-Up Radio Operation*; IEEE: Piscataway, NJ, USA, 2021; pp. 1–180. [[CrossRef](#)]
40. Mazloum, N.; Edfors, O. Interference-Free OFDM Embedding of Wake-Up Signals for Low-Power Wake-Up Receivers. *IEEE Trans. Green Commun. Netw.* **2020**, *4*, 669–677. [[CrossRef](#)]
41. Skrimponis, P.; Mirfarshbafan, S.H.; Studer, C.; Rangan, S. Power Efficient Multi-Carrier Baseband Processing for 5G and 6G Wireless. In Proceedings of the 2020 54th Asilomar Conference on Signals, Systems, and Computers, Pacific Grove, CA, USA, 1–5 November 2020; pp. 324–330. [[CrossRef](#)]
42. Third Generation Partnership Project R1-2407492. RAN1#118 Final Summary of Discussion on LP-WUS and LP-SS Design Vivo. 2024. Available online: https://www.3gpp.org/ftp/tsg_ran/WG1_RL1/TSGR1_118/Docs/R1-2407492.zip (accessed on 9 December 2024).
43. Third Generation Partnership Project R1-2409308. RAN1#118bis Final Summary of Discussion on LP-WUS and LP-SS Design Vivo. 2024. Available online: https://www.3gpp.org/ftp/tsg_ran/WG1_RL1/TSGR1_118b/Docs/R1-2409308.zip (accessed on 9 December 2024).
44. Wentzloff, D.D.; Alghaihab, A.; Im, J. Ultra-Low Power Receivers for IoT Applications: A Review. In Proceedings of the 2020 IEEE Custom Integrated Circuits Conference (CICC), Boston, MA, USA, 22–25 March 2020; pp. 1–8. [[CrossRef](#)]
45. Mercier, P.P.; Calhoun, B.H.; Wang, P.-H.P.; Dissanayake, A.; Zhang, L.; Hall, D.A.; Bowers, S.M. Low-Power RF Wake-Up Receivers: Analysis, Tradeoffs, and Design. *IEEE Open J. Solid-State Circuits Soc.* **2022**, *2*, 144–164. [[CrossRef](#)]
46. Razavi, B. *RF Microelectronics*, 2nd ed.; Prentice Hall Press: Saddle River, NJ, USA, 2011.
47. Moody, J.; Bassirian, P.; Roy, A.; Liu, N.; Barker, N.S.; Calhoun, B.H.; Bowers, S.M. Interference Robust Detector-First Near-Zero Power Wake-Up Receiver. *IEEE J. Solid-State Circuits* **2019**, *54*, 2149–2162. [[CrossRef](#)]
48. Roberts, N.E.; Craig, K.; Shrivastava, A.; Wooters, S.N.; Shakhsher, Y.; Calhoun, B.H.; Wentzloff, D.D. 26.8 A 236nW -56.5dBm-sensitivity bluetooth low-energy wakeup receiver with energy harvesting in 65nm CMOS. In Proceedings of the 2016 IEEE International Solid-State Circuits Conference (ISSCC), San Francisco, CA, USA, 31 January–4 February 2016; pp. 450–451. [[CrossRef](#)]
49. Shen, X.; Duvvuri, D.; Bassirian, P.; Bishop, H.L.; Liu, X.; Dissanayake, A.; Zhang, Y.; Blalock, T.N.; Calhoun, B.H.; Bowers, S.M. A 184-nW, -78.3-dBm Sensitivity Antenna-Coupled Supply, Temperature, and Interference-Robust Wake-Up Receiver at 4.9 GHz. *IEEE Trans. Microw. Theory Tech.* **2022**, *70*, 744–757. [[CrossRef](#)]

50. Wang, P.-H.P.; Jiang, H.; Gao, L.; Sen, P.; Kim, Y.-H.; Rebeiz, G.M.; Mercier, P.P.; Hall, D. A 400 MHz 4.5 nW -63.8 dBm sensitivity wake-up receiver employing an active pseudo-balun envelope detector. In Proceedings of the ESSCIRC 2017—43rd IEEE European Solid State Circuits Conference, Leuven, Belgium, 11–14 September 2017; pp. 35–38. [[CrossRef](#)]
51. Jiang, H.; Wang, P.-H.P.; Gao, L.; Sen, P.; Kim, Y.-H.; Rebeiz, G.M.; Hall, D.A.; Mercier, P.P. 24.5 A 4.5nW wake-up radio with -69 dBm sensitivity. In Proceedings of the 2017 IEEE International Solid-State Circuits Conference (ISSCC), San Francisco, CA, USA, 5–9 February 2017; pp. 416–417. [[CrossRef](#)]
52. Weinreich, S.; Murmann, B. A 0.6–1.8-mW 3.4-dB NF Mixer-First Receiver With an N-Path Harmonic-Rejection Transformer-Mixer. *IEEE J. Solid-State Circuits* **2023**, *58*, 1508–1518. [[CrossRef](#)]
53. Liu, R.; Asma Beevi, K.T.; Dorrance, R.; Dasalukunte, D.; Kristem, V.; Lopez, M.A.S.; Min, A.W.; Azizi, S.; Park, M.; Carlton, B.R. An 802.11ba-Based Wake-Up Radio Receiver With Wi-Fi Transceiver Integration. *IEEE J. Solid-State Circuits* **2020**, *55*, 1151–1164. [[CrossRef](#)]
54. Mirzaei, A.; Darabi, H.; Leete, J.C.; Chen, X.; Juan, K.; Yazdi, A. Analysis and Optimization of Current-Driven Passive Mixers in Narrowband Direct-Conversion Receivers. *IEEE J. Solid-State Circuits* **2009**, *44*, 2678–2688. [[CrossRef](#)]
55. Andrews, C.; Molnar, A.C. A Passive Mixer-First Receiver With Digitally Controlled and Widely Tunable RF Interface. *IEEE J. Solid-State Circuits* **2010**, *45*, 2696–2708. [[CrossRef](#)]
56. Dissanayake, A.; Moody, J.; Bishop, H.L.; Truesdell, D.; Muhlbauer, H.; Lu, R.; Gao, A.; Gong, S.; Calhoun, B.H.; Bowers, S.M. A- 108dBm Sensitivity, -28 dB SIR, 130nW to 41 μ W, Digitally Reconfigurable Bit-Level Duty-Cycled Wakeup and Data Receiver. In Proceedings of the 2020 IEEE Custom Integrated Circuits Conference (CICC), Boston, MA, USA, 22–25 March 2020; pp. 1–4. [[CrossRef](#)]
57. Moosavifar, M.; Im, J.; Odelberg, T.; Wentzloff, D. A 110 μ W 2.5kb/s -103 dBm-Sensitivity Dual-Chirp Modulated ULP Receiver Achieving -41 dB SIR. In Proceedings of the 2022 IEEE International Solid-State Circuits Conference (ISSCC), San Francisco, CA, USA, 20–26 February 2022; pp. 402–404. [[CrossRef](#)]
58. Shirazi, A.H.M.; Lavasani, H.M.; Sharifzadeh, M.; Rajavi, Y.; Mirabbasi, S.; Taghivand, M. A 980 μ W 5.2dB-NF current-reused direct-conversion bluetooth-low-energy receiver in 40nm CMOS. In Proceedings of the 2017 IEEE Custom Integrated Circuits Conference (CICC), Austin, TX, USA, 30 April–3 May 2017; pp. 1–4. [[CrossRef](#)]
59. Selvakumar, A.; Zargham, M.; Liscidini, A. 13.6 A 600 μ W Bluetooth low-energy front-end receiver in 0.13 μ m CMOS technology. In Proceedings of the 2015 IEEE International Solid-State Circuits Conference—(ISSCC) Digest of Technical Papers, San Francisco, CA, USA, 22–26 February 2015; pp. 1–3. [[CrossRef](#)]
60. Odelberg, T.J.; Im, J.; Moosavifar, M.; Wentzloff, D.D. A Fully Integrated NB-IoT Wake-Up Receiver Utilizing An Optimized OFDM 12-Point FFT Wake-Up Engine. In Proceedings of the 2024 IEEE International Symposium on Circuits and Systems (ISCAS), Singapore, 19–22 May 2024; pp. 1–5. [[CrossRef](#)]

Disclaimer/Publisher’s Note: The statements, opinions and data contained in all publications are solely those of the individual author(s) and contributor(s) and not of MDPI and/or the editor(s). MDPI and/or the editor(s) disclaim responsibility for any injury to people or property resulting from any ideas, methods, instructions or products referred to in the content.